# Electric, dielectric and AC electrical conductivity study of $Al^{3+}$ substituted barium hexaferrite nanoparticles synthesized by Sol-gel auto-combustion technique

Vinod N. Dhage [a,*], Maheshkumar L. Mane [b], S.B. Rathod [c], S.M. Rathod [a], K.M. Jadhav [d]

[a] Department of Physics, MES Abasaheb Garware College, Pune (M.S.) 411 004, India
[b] S.G. R.G.Shinde Mahavidyalaya, Paranda, Osmanabad (M.S.) 413 502, India
[c] Waghire College of Arts, Commerce and Science, Saswad, Purandar (M.S.) 412 301, India
[d] Department of Physics, Dr.Babasaheb Ambedkar Marathwada University, Aurangabad (M.S.) 431 004, India

## ARTICLE INFO

## ABSTRACT

$Al^{3+}$ substituted barium hexaferrite $BaFe_{12-x}Al_xO_{19}$ (where $\times$ x = 0.00, 0.25, 0.50, 0.75,1.00) nanoparticles have been prepared by sol–gel auto combustion technique. Two probe method is used to study the electrical resistivity and dielectric properties of aluminium substituted barium hexaferrite. The DC electrical resistivity reveals that the electrical resistivity as well as the activation energy increases with increase in $Al^{3+}$ content x. On the basis of Maxwell-Wagner and Koop's theory the dielectric parameters such as dielectric constant ($\varepsilon'$), dielectric loss ($\varepsilon''$) and dielectric loss tangent (tan$\delta$) with frequency are discussed. The dielectric parameters decreases with increase in $Al^{3+}$ content x. The room temperature AC electrical conductivity measurements were carried out at different frequencies (20 Hz –1 MHz). The experimental results indicate that AC electrical conductivity ($\sigma_{ac}$) increases with increase in the frequency, indicating semiconducting behaviour of the samples. The AC impedance spectroscopy technique is used to study internal grain resistance and grain boundary distribution of the prepared aluminium substituted barium hexaferrite samples.

© 2021 Elsevier Ltd. All rights reserved.
Selection and peer-review under responsibility of the scientific committee of the International Web Conference on Advanced Materials Science and Engineering.

## 1. Introduction

The broad range of synthetic and investigative techniques from chemistry, Physics and Material science, scientists and technologists are attracted towards the magnetic nanoparticles [1,2]. Among these magnetic materials, M−type barium hexaferrite ($BaFe_{12}O_{19}$) have been intensively studied recently considering the excellent characteristics and their potential applications such as high resistance, superior chemical stability, powerful corrosion, good mechanical hardness, high level of signal to noise ratio, high Coercivity, large single axis anisotropy, high-density magnetic recording, electronic devices [3-7]. The M−type barium hexaferrite have good mechanical, chemical stability and high microwave magnetic loss [8,9]. Many synthesis methods are implemented for the preparation of hexaferrite nanoparticles such as sol–gel

auto combustion [10,11],chemical co-precipitation[12], Hydrothermal [13], microemulsion [14],glass crystallization [15], Citrate precursor [16] and reverse micelle technique[17].The sol–gel auto combustion technique was widely used to prepare nanocrystalline barium hexaferrite, due to simple process and the controllable stoichiometric amounts [18]. Highly pure multi-component oxides were synthesized by chemical route. Potential advantages of the wet chemical route over the conventional solid state reaction method include better homogeneity, better compositional control and lower processing temperatures [19]. We have synthesized aluminium substituted barium hexaferrite nanoparticles by sol–gel auto combustion technique. Sol–gel auto combustion is a novel method, with a unique combination of the chemical sol–gel process and the combustion process, based on the gelling and subsequent combustion of an aqueous solution of the desired metals and some organic fuel.

Hexaferrite plays an important role in the field of electronic industry due to their magneto-dielectric properties. Due to the

* Corresponding author.
  E-mail address: drvinoddhage.agc@gmail.com (V.N. Dhage).

*V.N. Dhage, M.L. Mane, S.B. Rathod et al.*

prominent properties such as low cost, easily manufacturing, and interesting electric, dielectric and magnetic properties lead the polycrystalline ferrite important candidate in the field of technological applications. These materials are categorized into magnetic semiconductors. A few studies are available on electrical conductivity, thermal conductivity and dielectric properties for the hexagonal ferrites [20,21]. The electrical and dielectric properties of magnetic materials is depend on the preparation conditions, such as sintering temperature, sintering atmosphere, and soaking time as well as the type of substituted ions [22].

Study of the effect of frequency, composition on the dielectric properties and the dc electrical resistivity offers much valuable information on the behaviour of the localized electric charge carriers which can lead to a good explanation and understanding of the mechanism of electric conduction and dielectric polarization in ferrite systems [23]. The structural and magnetic properties of $Al^{3+}$ substituted $BaFe_{12}O_{19}$ nanoparticles have been discussed in our previous report [24]. The trivalent substituted barium hexaferrite samples have been studied by researchers [25,26] but it's electric and dielectric properties of aluminium substituted barium hexaferrite with same composition have not been studied in detail by the researchers as per our knowledge. The motivation to substitute $Al^{3+}$ inplace of $Fe^{3+}$ ions is that as aluminium is good conducting and nonmagnetic ion so to study the effect of aluminium doping on the electric and dielectric properties of barium hexaferrite have been carried out. The present work reports on the d.c electrical resistivity, dielectric constant ($\varepsilon'$), dielectric loss ($\varepsilon''$) and dielectric loss tangent (tan$\delta$), ac conductivity ($\sigma_{ac}$) and ac impedance spectroscopic properties of $Al^{3+}$ substituted barium hexaferrite samples.

## 2. Experimental

The nanocrystalline $Al^{3+}$ substituted barium hexaferrite samples were prepared by sol–gel auto-combustion technique. The details of the experimental procedure are given in our previous work [24]. The dc resistivity measurement of samples was done by two-probe method using silver paste as a contact material. For good surface contact the sample is firmly fixed between the two electrodes. The chromel–alumel thermocouple was used to measure the temperature. The dielectric parameters were measured as a function of frequency using an LCR-Q meter (Model HP 4284). The dielectric measurements as a function of frequency were made using two-probe method at the frequency range of 20 Hz to 1 MHz at room temperature.

## 3. Results and discussion

### 3.1. DC electrical resistivity

The electrical property of the ferrite materials depends upon chemical composition, methods of preparation, sintering temperature and grain size. DC electrical resistivity was measured by using two probe technique [27]. The samples were used in the form of pellets of 10 mm diameter and of 3 mm thickness. The pellets were prepared at room temperature by compressing at 6 tons pressure. The DC electrical resistivity of all the samples decreases with increase in the temperature in accordance with Arrhenius equation [27]

$$\rho = \rho_0 \exp\left(\frac{\Delta E_g}{K_B T}\right) \qquad (1)$$

Here 'ρ' is the resistivity at temperature 'T', $\rho_0$ is the pre exponential constant which equals the resistivity at infinitely high temperature; $K_B$ is the Boltzman's constant and $\Delta E$ is the activation

energy, which is the energy needed to release an electron from the ion for a jump to neighboring ion, giving rise to the electrical conductivity.

The Arrhenius plot of each sample is shown in Fig. 1. This plot shows decrease in resistivity with the rise in temperature, ensuring the semiconducting behavior of ferrites [28,29].The electrical resistivity decreases as sintering time increases the crystal growth enhanced [30,31]. Conduction in ferrites may be explained by Verwey's hopping mechanism [32]. According to Verwey, the electronic conduction in ferrites is mainly due to hopping of electrons between ions of same element present in more than one valance state, distributed randomly over the crystallographically equivalent lattice sites. The electron hopping between (A) and [B] sites under normal conditions therefore has a very small probability compared with that for [B –B] hopping. Hopping between (A) and (A) sites does not exists for the simple reason that there are only $Fe^{3+}$ ions at (A) site and any $Fe^{2+}$ ions form enduring processing preferentially occupy [B] sites only. The hopping probability depends upon the separation between the ions involved and the activation energy [33]. The electrical resistivity increases with increase in aluminium content × as shown in Fig. 1. Similar results were obtained for Al-Ga [34] and $Pb^{3+}$[22] substituted strontium hexaferrite samples. The activation energy of each sample in the measured temperature range can be determined from the slope of the linear plots as shown in Fig. 1. The values of activation energy at ferrimagnetic region ($E_f$), paramagnetic region ($E_p$) and $\Delta E$ ($E_p$-$E_f$) are shown in Table 1. From Table 1 it is observed that the activation energy at paramagnetic region ($E_p$) is greater than activation energy at ferrimagnetic region ($E_f$). The activation energy ($\Delta E$) is greater than approximately 0.2 eV, which according to Klinger [35] suggests that the conduction is due to polaron hopping. The hopping mechanism depends on the activation energy, which is associated with the electrical energy barrier experienced by the electrons during hopping. In addition to the above said considerations, the activation energy is influenced by the grain size, as grain size increases grain–grain contact area increases for the electron to flow and therefore there is a lower barrier height [31]. The standard error occurred in calculation of activation energy with intercept value 0.32146 ± 0.01055and slope value 0.09224 ± 0.01 723 was calculated from linear fit method.

The drift mobility ($\mu_d$) of all the samples have been calculated by using the relation [36],
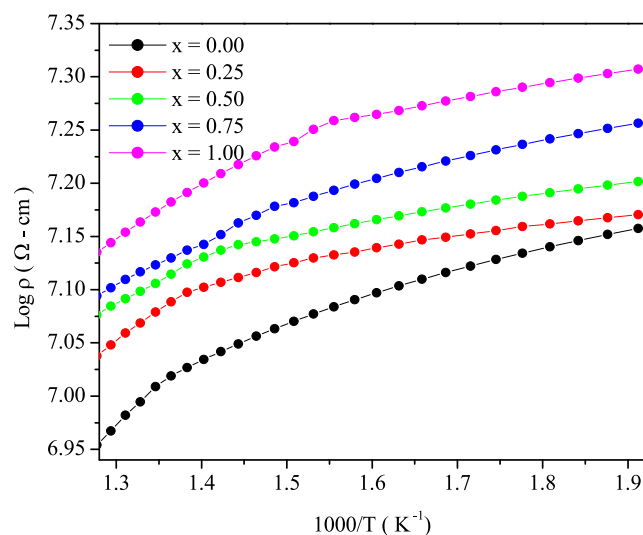


**Fig 1.** Variation of Log ρ versus 1000/T ($K^{-1}$) for $BaFe_{12-x}Al_xO_{19}$ Samples.

**Table 1**
Activation energy in paramagnetic region (E$_p$), ferrimagnetic region (E$_f$), E$_p$-E$_f$ (ΔE) and Curie temperature (T$_c$) for BaFe$_{12-x}$Al$_x$O$_{19}$ samples.

| Comp.x | E$_p$ (eV) | E$_f$ (eV) | ΔE (eV) | T$_c$ (K) |
|--------|-----------|-----------|---------|-----------|
| 0.00 | 0.71536 | 0.40776 | 0.3076 | 740 |
| 0.25 | 0.57164 | 0.21614 | 0.3555 | 718 |
| 0.50 | 0.50794 | 0.12677 | 0.3812 | 698 |
| 0.75 | 0.53232 | 0.14637 | 0.3859 | 681 |
| 1.00 | 0.51599 | 0.10822 | 0.4077 | 645 |

$$\mu_d = \frac{1}{\eta \, e \, \rho} \qquad (2)$$

Where e is the charge on electron, $\rho$ is the resistivity at particular temperature and $\eta$ is the concentration of charge carriers that can be calculated from the relation [37].

$$\eta = \frac{N_a \, \rho_m \, p_{Fe}}{M} \qquad (3)$$

where M is the molecular weight of the sample, N$_a$ is the Avogadro's number, $\rho_m$ is the apparent density of the sample and P$_{Fe}$ is the number of iron atoms in the chemical formula of the oxide sample. It can be seen that the resistivity and drift mobility are the inverse physical quantities, the samples having low resistivity have higher mobility and vice versa [38]. To examine the temperature dependence of the drift mobility a graph between drift mobility ($\mu_d$) and 1000/T is shown in Fig. 2.The drift mobility decreases with increase in aluminium content x. It can be observed from Fig. 2 the drift mobility increases with increase in temperature, it may be due to the hopping of charge carriers from one site to another site [38].

### 3.2. Frequency dependence of dielectric parameters

The dielectric constant of the prepared nanocrystalline aluminium substituted barium hexaferrite ($\varepsilon'$) is given by the following equation

$$\varepsilon' = \frac{C \, d}{\varepsilon_o A} \qquad (4)$$

Where C is the capacitance in farad, d is the thickness of the pellet in meter, $\varepsilon_0$ is the permittivity of free space and A is the area of the pellet. The room temperature frequency dependence of dielectric parameters for all the samples have been studied. The dielectric properties of aluminium substituted barium hexaferrite are influenced by various factors such as method of preparation, sintering condition, chemical composition, ionic charge and particle size etc. The variation of dielectric constant ($\varepsilon'$) with logarithm of frequency (log f) is shown in Fig. 3. From Fig. 3 it is seen that the dielectric constant ($\varepsilon'$) decreases rapidly with increase in frequency and at higher frequency it remains almost constant. The conduction process in materials is similar to mechanism discussed by Rabinkin and Novikova for polarization in ferrites. Polarization decreases with increase in frequency and then reaches to a constant value due to the fact that beyond a certain frequency of external field, the electron exchange between Fe$^{2+}$ and Fe$^{3+}$ cannot follow the alternating field [39].The large value of $\varepsilon'$ at lower frequency is due to the predominance of species like Fe$^{2+}$ ions [40]. However the decreasing behaviour of $\varepsilon''$ with frequency is natural because of the fact that any species contributing to polarizability lags behind the applied field at higher and higher frequencies.

The decrease in the values of tanδ and with the frequency is a normal behaviour for ferrites and can be explained on the basis of charge polarization. The phenomenon of charge polarization is a result of the presence of higher conductivity phase (grains) in the insulating matrix (grain boundaries) of a dielectric, causing localized accumulation of charge under the influence of electric field. The reduction in dielectric loss tangent (tanδ) occurs since the frequency of hopping of electron exchange between Fe$^{2+}$ and Fe$^{3+}$ is far from the frequency of the alternating electric field.

Fig. 4 shows the variation of dielectric loss tangent (tanδ) as a function of frequency for Al$^{3+}$substituted barium hexaferrite samples. The decrease in tanδ takes place when the jumping rate of charge carriers lags behind the alternating electric field beyond a certain critical frequency. From Fig. 4 it is seen that for all the samples tanδ decreases continuously with increasing frequency. The values of dielectric loss tangent depends on number of factors such as stoichiometry, Fe$^{2+}$ content and structural homogeneity which in turn depends on the composition and sintering temperature of the samples [41].Thus the tangent of dielectric loss angle of ferrite nanoparticles is expected to decrease approximately inversely as frequency. In the low frequency region which corresponds to high resistivity (due to grain boundary) more energy is required for electron exchange between Fe$^{2+}$ and Fe$^{3+}$ ions. Thus the energy loss is high. The resistive grain boundaries were found to be more effective at lower frequencies while the conductive ferrite grains are
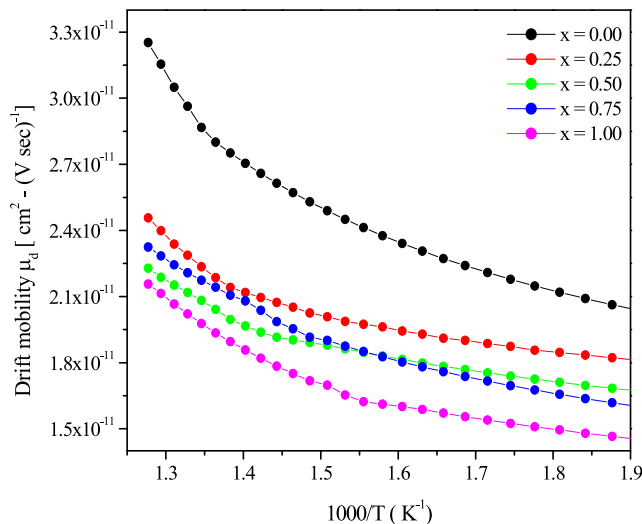


**Fig 2.** Variation of drift mobility ($\mu_d$) with 1000/T (K$^{-1}$) of BaFe$_{12-x}$Al$_x$O$_{19}$ samples.
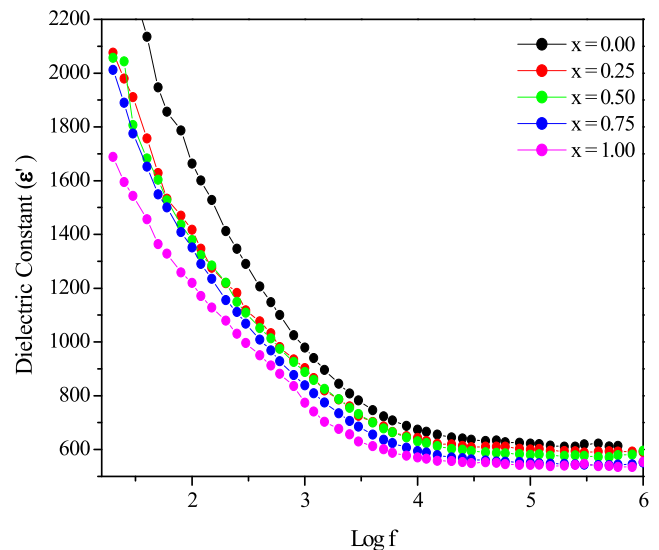


**Fig 3.** Variation of Dielectric Constant ($\varepsilon'$) with Log f of BaFe$_{12-x}$Al$_x$O$_{19}$ samples.

V.N. Dhage, M.L. Mane, S.B. Rathod et al.
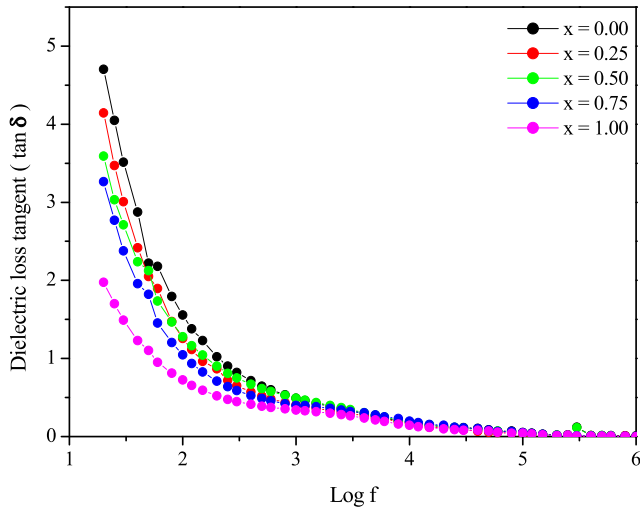
**Fig 4.** Variation of dielectric loss tangent (tanδ) with Logf of $BaFe_{12-x}Al_xO_{19}$ samples.

more effective. In the high frequency range which corresponds to low resistivity. (Due to grain) a small energy is needed for electron transfer between $Fe^{2+}$ and $Fe^{3+}$ in the grains and hence the energy loss is small. The dielectric loss was determined using Eq. (5).

$$\varepsilon'' = \varepsilon' \tan \delta \qquad (5)$$

Where $\varepsilon'$ is the dielectric constant, $\tan \delta$ is the dielectric loss tangent and $\varepsilon''$ is the dielectric loss of the prepared nanomaterials. Dielectric loss is an important part of the total core loss in ferrites [42]. Fig. 5 shows the variation of dielectric loss as a function of frequency for all the compositions. Hudson [43] has shown that the dielectric losses in ferrite are generally reflected in the conductivity measurements where the materials of high conductivity exhibit high losses and vice versa.

### 3.3. AC conductivity

The AC conductivity shows an increasing trend with the increase in frequency for all the samples. This behaviour is - similar to the Maxwell–Wagner type. The dielectric structure of ferrites is given by Koop's phenomenological theory and Maxwell – Wagner theory [44,45]. The plots of AC conductivity are linear,

indicating that the conduction is attributed to small polarons, as reported by Alder and Fienleib [46]. At higher frequencies, where conductivity increases greatly with frequency, the transport is dominated by contributions from hopping infinite clusters. The electrical conductivity in ferrite is mainly due to hopping of electrons between ions of the same element present in more than one oxidation state, distributed randomly over crystallographically equivalent lattice sites. The hopping between tetrahedral and octahedral has very small probability compared with that for octahedral – octahedral hopping. The hopping between tetrahedral–tetrahedral sites does not exist, due to that there are only $Fe^{3+}$ ions at tetrahedral sites and any $Fe^{2+}$ ions form enduring sintering process preferentially occupy octahedral sites only.

The AC conductivity of $BaFe_{12-x}Al_xO_{19}$ with x = 0.00–1.00 in steps of 0.25 is shown in Fig. 6. It is well known that the dielectric constant ($\varepsilon'$), dielectric loss ($\varepsilon''$), dielectric loss tangent (tanδ) and AC electrical conductivity ($\sigma_{ac}$) are electrical properties and exchange of electrons between $Fe^{2+}$ and $Fe^{3+}$ ions are responsible for the conduction mechanism. From the dielectric loss and dielectric permittivity, AC conductivity of ferrite samples can be evaluated using the relation [47]

$$\sigma_{AC} = 2\pi \varepsilon_o \varepsilon' f \tan \delta \qquad (6)$$

Where 'f' is the frequency of the applied field, $\varepsilon_o$ is the permittivity of free space, $\varepsilon'$ is the real part of relative permittivity of the samples, and tanδ is the dielectric loss tangent and $\sigma_{AC}$ is the ac conductivity of the samples [41]. From the Fig. 6 it is observed that AC conductivity decreases with increase in composition x. It is observed that, at varying frequency, the dielectric constant of x= 0.00 is higher than those of x= 1.00. tant of x = 0.00 is higher than those of × = 1.00. This is because of electrode effects in parallel capacitance geometry of dielectric measurements.

### 3.4. AC impedance

The AC impedance analysis provides platform to separate out the bulk and grain boundary contribution to the total conductivity. The impedance spectrum is usually represented as real component of impedance (Z') versus real imaginary component of impedance (Z''), which is referred, as Nyquist plot. The semicircles at higher and lower frequencies represent bulk and electrode process, respectively, while that at intermediate frequencies represents grain boundary contribution [48].
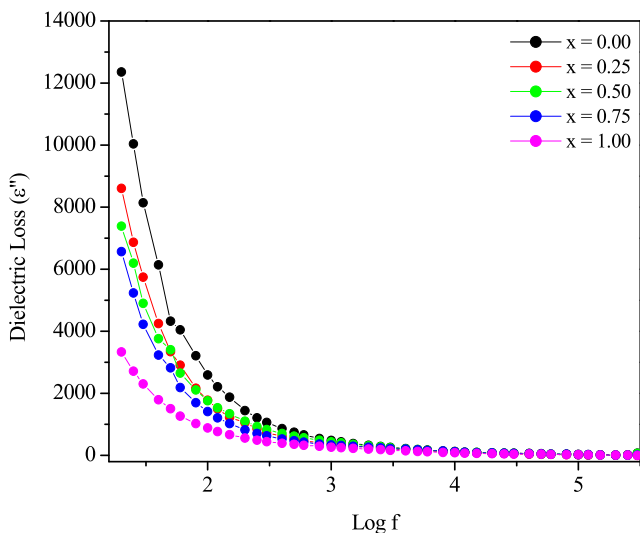


**Fig 5.** Variation of dielectric loss ($\varepsilon''$) with Log f of $BaFe_{12-x}Al_xO_{19}$ samples.
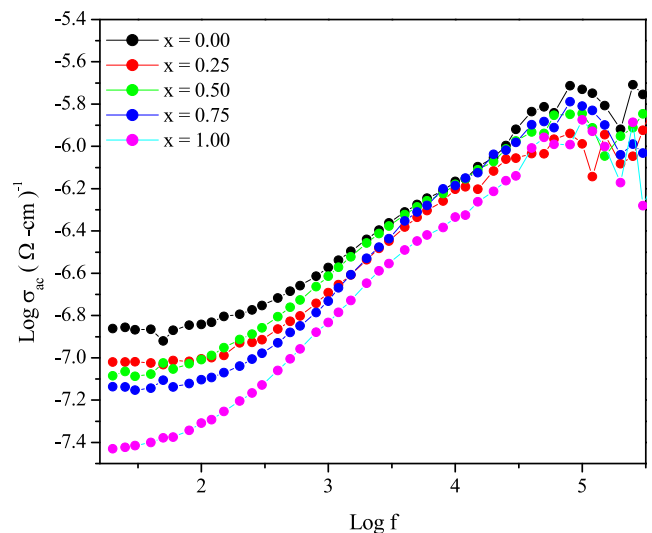


**Fig 6.** Variation of ac conductivity ($\sigma_{ac}$) with Log f of $BaFe_{12-x}Al_xO_{19}$ samples.

V.N. Dhage, M.L. Mane, S.B. Rathod et al.
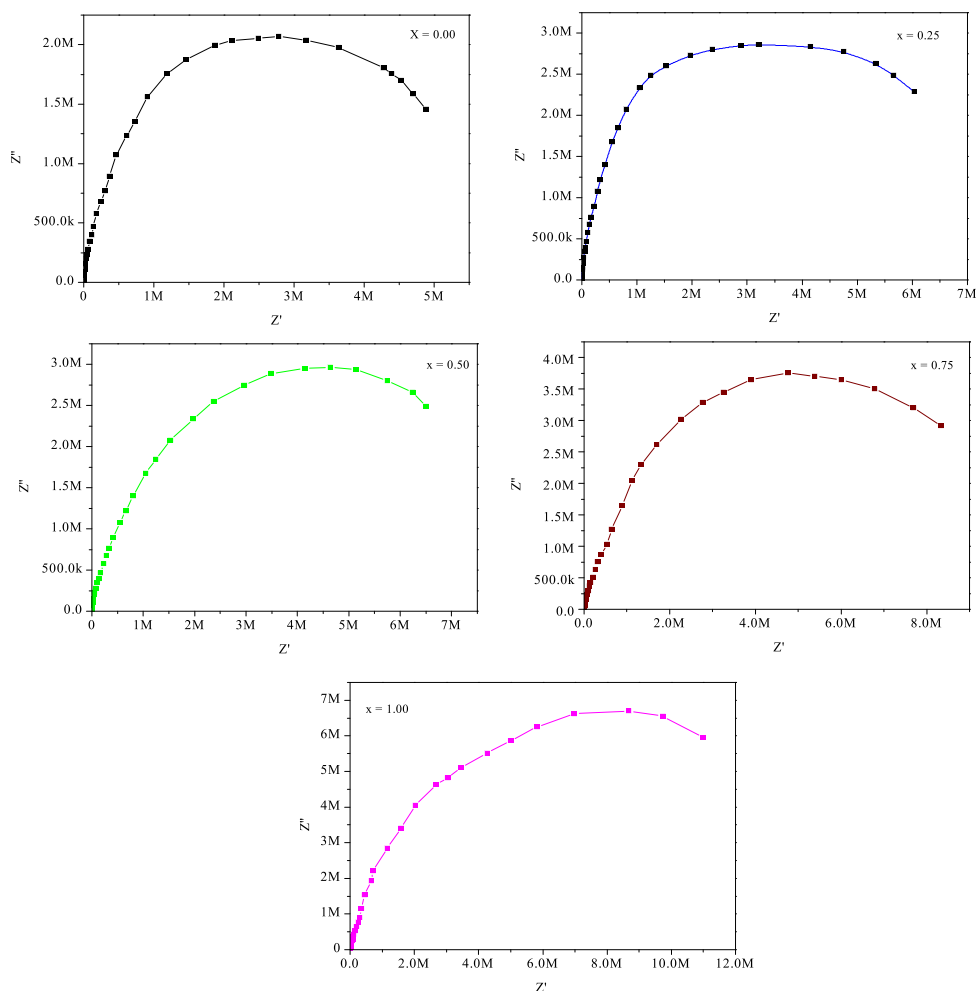
**Fig 7.** Nyquist plots for $BaFe_{12-x}Al_xO_{19}$ samples.

Fig. 7 shows the variation of the real part (Z′) and the imaginary part (Z″) of complex impedance as a function of applied frequency for $BaFe_{12-x}Al_xO_{19}$ (where x = 0.00, 0.25, 0.50, 0.75, 1.00) samples recorded at room temperature. The value of Z″ initially increases and reaches maximum value and then decreases forming semicirclein the frequency range of 20 Hz – 1 MHz. The size of the semicircle depends on the grain size and the number of grains present in the material. The presence of single semicircular obtained at higher frequencies corresponds to electrical conduction by the interior of the grain, the diameter of the semicircle is corresponds to the resistance of that grain [49]. As the aluminium content increases the diameter of the semicircle goes on increasing which indicates increase in grain interior resistance. Thus the total impedance (Z′, the real axis intercepts at low frequency side) and imaginary component of complex impedance Z″ of aluminium substituted barium hexaferrite increases with increase in $Al^{3+}$ substitution x.

## 4. Conclusions

$BaFe_{12-x}Al_xO_{19}$ (where x = 0.00 – 1.00 in step of 0.25) nanoparticles have been successfully prepared by sol–gel auto combustion technique. As $Al^{3+}$ substitution x increases DC resistivity increases. The activation energy in ferrimagnetic region is lower than that of paramagnetic region. The Curie temperature obtained from DC electrical resistivity decreases with increase in aluminium content × and it is in the reported range. The dielectric constant (ε′),

dielectric loss (ε″), dielectric loss tangent (tanδ) decreases with increase in $Al^{3+}$ substitution x. AC electrical conductivity decreases with increase in $Al^{3+}$content x. AC impedance spectroscopy allowed us to study the influence of grain size in the impedance response of nanocrystalline aluminium substituted barium hexaferrite. The total impedance (Z′, the real axis intercept at low frequency side) and imaginary part of complex impedance (Z″) of all samples is decreased with increase in aluminium concentration x. Thus, the substitution of aluminium in barium hexaferrite matrix strongly influences it's electrical and dielectric properties.

## Declaration of Competing Interest

The authors declare that they have no known competing financial interests or personal relationships that could have appeared to influence the work reported in this paper.

## Acknowledgement

## References

[1] S.M. El-Sayed, T.M. Meaz, M.A. Amer, H.A. El Shersaby, J. Physica B: Cond. Mat. 426 (2013) 137–143.
[2] S. Kumar, S. Supriya, M. Kar, J. Appl. Phys. 122 (2017) 224106.

[3] H. Kojima, in: E.P. Wolhfarth (Ed), Ferromagnetic Materials, Vol. 3, North-Holland Publishing, 1982, p.305.

[4] Ying Liu, Michael G.B. Drew, Yue Liu, Jingping Wang, Milin Zhang, J. Magn. Magn.Mater. 322 (2010) 814–818.

[5] M.A. Almessiere, B. Unal, Y. Slimani, A. Demir Korkmaz, N.A. Algarou, A. Baykal, Results in Physics 14 (2019) 102468.

[6] C.L. Dube, S.C. Kashyap, D.K. Pandya, D.C. Dube, J. Phys. Status Solidi A 206 (2009) 2627.

[7] S. Pratap Behera, J. Ravi, Solid State Sciences 89 (2019) 139–149.

[8] T. Nakamura, J. Appl. Phys. 88 (2000) 348–351.

[9] X.F. Pan, J.X. Qiu, M.Y. Gu, J. Mater. Sci. 42 (2007) 145–148.

[10] V.C. Chavan, S.E. Shirsath, M.L. Mane, R.H. Kadam, S.S. More, J. Magn. Magn. Mater. 398 (2016) 32–37.

[11] M. Han, Yu ou, Wenbing Chen, Longjang Deng, J. Alloys. Compd. 474 (2009) 185–189.

[12] K. SheikhiMoghaddam, A. Ataie, J. Alloys. Compd. 426 (2006) 415–419.

[13] MihaDrofenik, Irena ban J.Mat. Chem. and Phys. 127 (3) (2011) 415–419.

[14] X. Liu, J. Wang, L.M. Gan, S.C. Ng, J. Ding, J. Magn. Magn. Mater. 184 (1998) 344–354.

[15] L. Rezlescu, E. Rezlescu, P.D. Popa, N. Rezlescu, J. Magn. Magn. Mater. 193 (1999) 288–290.

[16] V.K. Sankaranarayanan, D.C. Khan, J. Magn. Magn. Mater. 153 (1996) 337–346.

[17] Xu. Ping, Xijiang Han, Maoju Wang, J. Phys. Chem. C 111 (2007) 5866–5870.

[18] Varsha.C. Chavan, Sagar E. Shirsath, Maheshkumar L. Mane, Surendra S. More, J. Chem. Pharm. Res. 7(4) (2015) 675–678.

[19] M. Kakihana, J. Sol-Gel Sci. Tech. 6 (1996) 7–55.

[20] S. Hussain, M.A. Rehman, A. Maqsood, M.S. Awan, J. Cryst. Growth. 297 (2006) 403–410.

[21] S. Hussain, A. Maqsood, J. Magn. Magn. Mater. 316 (2007) 73–80.

[22] AsghariMaqsood ShahidHussain, J. Alloys. Compd. 466 (2008) 293–298.

[23] M.A. El Hiti, J. Magn. Magn. Mater. 192 (1999) 305–313.

[24] Vinod N. Dhage, M.L. Mane, A.P. Keche, C.T. Birajdar, K.M. Jadhav, J.Phys. B: Condens. Matter. 406 (2011) 789 – 793.

[25] R.C. Alange, Pankaj P. Khirade, Shankar D. Birajdar, Ashok V. Humbe, K.M. Jadhav, J. Mol. Struct. 1106 (2016) 460–467.

[26] T.M. Meaz, C. Bender Koch, Hyperfine Interact. 166 (2005) 455–463.

[27] M.J. Iqbal, M.N. Ashiq, P.H. Gomez, J.M. Munoz, J. Magn. Magn. Mater. 320 (2008) 881–886.

[28] J. Smit, H.P.J. Wijin, Ferrites, Wiley, NewYork, 1959.

[29] M.A. Ahmed, M.A. El. Hiti, J. Phys. III France 5 (1995) 776.

[30] A.M. El-Rafae, EnergyJ. Sol. 23 (1) (2000) 93–96.

[31] A. Verma, O.P. Thakur, C. Prakash, T.C. Goel, R.G. Mandivatta, J. Mater. Sci. Eng. B 116 (2005) 1–6.

[32] E.J.W. Verwey, J.H. De Boer, Rec. Trans. Chim. Des. Pays. Bas 55 (1936) 531.

[33] A. Lakshman, P.S.V. SubaRao, B.P. Rao, K.H. Rao, J. Phys. D 38 (2005) 673–678.

[34] Muhammad NaeemAshiq MuhammedJavedIqbal, Pablo Hernandez-Gomez, Jose Maria Munoz, J. Magn. Magn. Mater 320 (2008) 881–886.

[35] M.I. Klinger, J. Phys. C 8 (1975) 3595.

[36] M. Barakat, M.A. Henaish, S.A. Olofa, A. Twafik, J. Therm. Anal. 37 (1991) 241–248.

[37] N.F. Mott, E.A. Davis, Electronic Processesing Non-Crystalline Material, Clarendon press, Oxford London, 1979.

[38] U. Islam, I. Ahmad, T. Abbas, M. A. Chaudhry, R. Nazmeen, Proceedings of the 6th InternationalSymposium,1999, p.155.

[39] I.T. Rabinkin, Z.I. Novikova, Ferrites IZV Acad. Nauk USSR Minsk (1960) 146.

[40] J.C. Maxwell, Electric and Magnetism Vol. 2 (1973) 828.

[41] S.M. El-Syed, T.M. Meaz, M.A. Amer, H.A. ElShersaby, Physica B 426 (2013) 137–143.

[42] J. Zhu, K.J. Tseng, C.F. Foo, IEEE Trans. Magn. 36 (2000) 3408–3411.

[43] A.S. Hudson, Marconi Rev. 37 (1968) 43.

[44] C.G. Koops, Phys. Rev. 83 (1951) 121.

[45] K.W. Wagner, Am. Phys. 40 (1973) 317.

[46] D. Alder, J. Fienleib, Phys. Rev. B 2 (1970) 3112.

[47] R.C. Kambale, P.A. Shaikh, C.H. Bhosale, K.Y. Rajpure, Y.D. Kolekar, J. Smart. Mater. Struct. 18 (2009) 085014–85020.

[48] M.G. Chourashiya, J.Y. Patil, S.H. Pawar, L.D. Jadhav, J. Mater. Chem. Phys. 109 (2008) 39–44.

[49] H. Ya, R.B. Jackman, P. Hing, J. Appl. Phys. 94 (2003) 7878.